[Frontiers in Bioscience E3, 326-340, January 1, 2011]

The effect of coptis chinensis on the signaling network in the squamous carcinoma cells

Hongxia Wang[1], Fengchun Zhang[2], Fei Ye[3], Yuan Ma[1], David Y Zhang[3]

[1]Shanghai Renji Hospital, Shanghai Jiaotong University School of Medicine, China, [2]Suzhou Jiulong Hospital, Shanghai Jiaotong University School of Medicine, China, [3]Mount Sinai School of Medicine, New York University, USA

TABLE OF CONTENTS

1. ABSTRACT

The effects of Coptis chinensis on the behavior of squamous cell carcinoma have not yet been established. We examined the anticancer activity of Coptis chinensis on human squamous carcinoma cells, both *in vitro* and in xenografted nude mice, and applied Pathway Array Technology to understand possible involvement of signaling pathways in Coptis Chinensis induced tumor cells inhibition as well. Following Coptis chinensis treatment, a time-dependent reduction in proliferation was observed in both cell lines and NCR/NU mice. Coptis chinensis has a wide effect on cell signaling, including cell cycle regulation (Cdk6, Cdk4, cyclin B1, cyclin E, cyclin D1, p27), cell adhesion (E-cadherin, osteopontin), differentiation, apoptosis(p-Stat3, p53, BRCA1), cytoskeleton (p-PKC α/βII, Vimentin, p-PKCα), MAPK signaling (raf-1, ERK1/2, p-p38, p-ERK), and the phosphatidylinositol 3-kinase signaling pathway (p-Akt, Akt, p-PTEN). In our conclusions, Coptis chinensis may be a novel therapeutic drug for squamous cell carcinoma.

2. INTRODUCTION

Coptis chinensis is a traditional Chinese medicine (1). Historically, Coptis chinensis has been widely used in the treatment of inflammation diseases (2) and several skin diseases. Recently, several studies demonstrated that Coptis chinensis also has a strong anticancer activity. Hoshi *et al.* (3) initially reported that berberine, one of the main active alkaloids of Coptis chinensis, had a strong anti-proliferative effect on sarcoma-180 cells. Subsequently, it was found that Coptis chinensis inhibits different types of cancer cells, including sarcoma (4), hepatic (5), esophageal (6), and leukemic (7) cancer cells. Recently, we confirmed this inhibitory activity of Coptis chinensis on various cancer cells *in vitro*, including breast, lung, prostate, pancreatic, and squamous cancer cells. Furthermore, Coptis chinensis extract enhances the anticancer effect of other conventional chemotherapeutic agents, including 5-FU and paclitaxel (8). Therefore, Coptis chinensis would be a potential anticancer agent for various cancers for use either alone or in combination with other chemotherapeutic agents.

The mechanism of the actions of Coptis chinensis is still unclear. Kim *et al.* (9) reported that berberine can efficiently inhibit growth by inducing cell cycle arrest in anoikis-resistant MCF-7 and MDA-MB-231 cells. Ma *et al.* (7) demonstrated that Coptis chinensis induces the apoptosis of human leukemic U937 cells via the changes in the cytokine profile and protein expressions in the mitochondria pathway. Fukuda *et al.* (10) demonstrated that Coptis chinensis can inhibit Cox-2 transcriptional activity in colon cancer cells. Recently, Coptis chinensis has been shown to exert anti-metastatic properties in non-small lung cancer cells (11), to inhibit growth, and induce G1 cell cycle arrest followed by apoptosis in human epidermoid carcinoma A431 cells (12). It has also been shown to enhance the As_2O_3-mediated reduction in motility and invasion of glioma cells (13). However, whether these activities are responsible for its anticancer effect is still questionable.

Recently, genome profiling of differential gene expression using a microarray has been widely used. However, mRNA levels do not always accurately reflect the corresponding protein levels and do not reveal epigenetic changes in the posttranscriptional modulation of proteins (e.g., phosphorylation) or changes in protein degradation rates. Moreover, the mRNA expression profile does not reflect the complex network of protein-protein interaction and cell signaling that control cell function, such as proliferation and apoptosis. To better understand the molecular mechanisms of Coptis chinensis's effect on cell growth, we performed a global screening of signaling pathways using a Pathway Array Technology to map protein-protein interaction, systematically. The Pathway Array Technology is a powerful tool for analyzing changes in intracellular protein expression and phosphorylation in major cell signaling pathways, including cell proliferation, apoptosis, and stress response. More importantly, the Pathway Array system can assist in identifying global functional changes in the complex signaling network that drives cellular behavior. This will allow us to identify signature patterns and to identify mechanistic details about the underlying workings of the signaling network in Coptis chinensis.

This study was undertaken to determine the anticancer activity of Coptis chinensis on human squamous carcinoma cells both *in vitro* and in xenografted nude mice. Since berberine is one of the major active components of Coptis chinensis, we used berberine as a comparison to determine whether the purified molecules of Chinese medicines, in addition to the complex itself, have the same effect on cell signaling and to better understand the complex phytopharmacology of these drugs and avoid contradictory results. We applied Pathway Array Technology to compare the levels of proteins using 122 antibodies, map protein-protein interaction systematically, and to understand possible involvement of signaling pathways in Coptis chinensis -induced tumor cells inhibition. The information generated from this study will help to support the development of human clinical trials in the future.

3. METHODS AND MATERIALS

3.1. Cell lines, culture

Two human squamous cell carcinoma cell lines (KB and SCC-25) were purchased from American Type Culture Collection (Manassas, VA). The rationale of using two cell lines is that squamous cell carcinoma is a heterogeneous cancer and there may be a difference in their response to drugs.

KB, a human epidermoid carcinoma cell line; SCC-25, a human tongue squamous carcinoma cell line were cultured in a 1:1 mixture of DMEM (ATCC, Manassas, VA)/Ham's F12 (Mediatech, Manassas, VA) supplemented with 10% FBS (Life Technologies, Carlsbad, CA.), 1% Pen-Strep (Life Technologies, Carlsbad, CA.) and 400 ng /ml hydrocortisone (BD Biosciences, Bedford, MA). All cells were incubated at 37°C in a humidified atmosphere, containing 5% CO_2.

3.2. Chemicals and drugs

Coptis chinensis (rhizome) was obtained from Yifang Pharmaceutical Co., Ltd (Guangdong, China). The extract was dissolved in culture medium to 20 mg/ml, vortexed at room temperature for 1 min, and incubated at 37°C for 1 hour. This solution was centrifuged at 5,000 rpm for 10 minutes to remove any insoluble ingredients. The supernatant was passed through a 0.22-μm filter for sterilization and diluted with culture medium to final concentrations of 20-800 μg/ml.

Berberine ($C_{20}H_{18}C_lNO_4$) was purchased from Sigma (Sigma, St. Louis, MO). 10mM stock solution of berberine were prepared with DMSO (Sigma), and diluted with culture medium to a final concentration of 20-200 μM. For consistency, the same batch was used throughout the entire study. Control cells received DMSO (0.25%) or culture medium only.

3.3. Determination of cell viability

An MTT assay was used to determine the viability of KB and Scc-25 cells. Approximately 5×10^3 cells were seeded in each well of a 96-well plate and incubated for 24 hours. The cells were then treated with various concentrations of Coptis Chinensis and berberine. The cells were then cultured for 48 hours at 37°C. After treatment, 10μl of MTT (3, 4, 5-dimethylthiazol-2, 5-diphenyltetrazolium bromide: Sigma, St. Louis, MO) at a concentration of 5 mg/ml was added to each well. The cells were incubated for an additional 3 hours and the supernatant was discarded. Finally, 100μl of DMSO was added to the wells to dissolve the precipitate. Optical density (OD) was measured at a wavelength of 570 nm using an ELx800 (Bio-Tek Instruments, Inc., Winooski, VT).

3.4. Pathway Array

Cells in 10 cm dishes were washed twice with ice-cold PBS. Total cellular proteins were extracted from KB and Scc-25 cells using a lysis buffer containing 20mmol/L Tris-HCl (pH 7.5), 20mmol/L sodium Pyrophosphate, 40mmol/L B-glycerophosphate, 30mmol/L Sodium Fluoride, 2mmol/L EGTA, 10mmol/L NaCl, and

0.5% NP-40. After adding 200μl lysis buffer, the cell monolayer was removed from the dish using scraper. The lysate was sonicated three times for 15 seconds each time, and then centrifuged (14,000rpm, 30 minutes, 4°C). The tubes were kept on ice throughout the process. The protein concentration was determined with the BCA Protein Assay kit (PIERCE, Rockford, IL). Isolated proteins were separated by SDS-PAGE (10% acrylamide). Cell extract containing 300μg of protein was loaded in one well across the entire width of gel. After running the gel, the proteins were then transferred electrophoretically to a nitrocellulose membrane. After transfer, the membrane was blocked for 1 hour with 5% milk or 3% BSA. Next, the membrane was clamped with Mini-PROTEAN II Multiscreen apparatus that isolates 20 channels across the membrane (Bio-Rad, Hercules, CA). Two or three antibodies were added to each channel and allowed to hybridize overnight at 4□. Different sets of antibodies (templates 1 to 4) were used for each membrane. Polyclonal antibodies to p-EGFR, p-HER2/ErbB2, p-PDK1, p-PKCα/βII, p-PKCδ, p-p53, p-AKT, p-PTEN, p-RB, p-beta-catenin, p-stat5, p-Stat3, p-ERK, p-c-Kit, p-FGFR, p-eIF4B, p-ERK5, p-p90RSK, p-CREB, p-mTor, p-IGF-1 R/InsulinR, p-cdc2, p-c-Jun, p-SAPK/JNK, p-FLT3, p-p38, ERK, β-catenin, Akt, c-kit, eIF4B, Cleaved Caspase-3, VEGFR2, p-GSK-3α/β and monoclonal antibodies to p-p70 S6 Kinase, p-VEGFR Receptor2, p-IKB, p-Smad, Notch4, CREB, Stat1 and PDGF Receptor-beta were obtained from Cell Signaling Technology, Inc. (Beverly, MA). Polyclonal antibodies to p-Survivin, cyclinB1, cyclinD1, cyclinE, cdk6, cdc25B, cdk2, BRCA1, Cdk4, Neu, 14-3-3β, PKCα, EGFR, Wee1, cdc25C, Notch1, Trap, Bcl-2, HIF-1a, TTF-1, PTEN, SRC-1, p300, Bax, N-cadherin, cdc42, TNF-α, Vimentin, OPN, Survivin, E-cadherin, p16, WT1, NFkB p52, NFkB p50, Calretinin, p14 ARF, H-Ras, Bcl-6, NFkB p65, Myf-6, p15, ATR, FAS, SLUG, FGF-1, TDP1, FOXM1, Era, Syk, Eg5, Rad52, KLF6, CaMKKa, p-FAK, IL-1β, TERT, Rap1, HCAM, Lyn, Twist, patched, Erβ, VEGF, SK3, RhoB, Wnt-1 and monoclonal antibodies to β-tubulin, GAPDH, CHK1, MDM2, cdc2p34, E2F-1, PCNA, c-myc, FGFR-3, ETS1, p53, raf-1, p27, p21, p63, Mesothelin, ATF-1, K-Ras, α-tubulin, SUMO-1, MetRS, Ep-CAM, CD55, Rictor, CD59, Atm, ABCG2, Bad, TopoIIa, p38, Ub, PR, TRβ1, TRAIL, TAP, GLI-3, FGF-7 were obtained from Santa Cruz Biotechnology (Santa Cruz, CA). Monoclonal antibody to Hsp90 was obtained from Stressgen (Ann Arbor, MN). Polyclonal antibody to TGF-β and p-HGF R/c-MET were obtained from R&D Systems (Minneapolis, MN). Polyclonal antibody to p-PKCα, HIF-3α and HIF-2a were obtained from Upstate (Billerica, MA), Abcam (Cambridge, MA) and Novus Biologicals (Littleton, CO) separately. Monoclonal antibody to XIAP and Cox2 were obtained from BD Biosciences (Lexington, KY) and Cayman Chemical (Ann Arbor, MN) separately. The blot was washed and hybridized for 1 hour with secondary horseradish peroxidase-conjugated antibodies (Bio-Rad, Hercules, CA). Chemiluminescence signals were captured using the ChemiDoc XRS System. Differences in protein level are estimated by densitometric scanning and normalized using internal standards.

3.5 Protein extraction and Western blot analysis

Cells were washed in PBS and lysed in a buffer containing 20mmol/L Tris-HCl (pH 7.5), 20mmol/L sodium Pyrophosphate, 40mmol/L B-glycerophosphate, 30mmol/L Sodium Fluoride, 2mmol/L EGTA, 100mmol/L NaCl, and 0.5% NP-40. After incubation on ice for 10 minutes and centrifugation at 14,000 rpm for 30 minutes, the supernatants were collected, and the protein concentration was determined with the Protein Assay kit (Bio-Rad). Protein (20μg) was electrophoresed through a 10% polyacrylamide gel under nonreducing conditions and transferred to a nitrocellulose membrane (Bio-Rad) by electroblotting. After transfer, the blots were incubated with first antibodies on a shaker at 4°C overnight. The membranes were then washed with TBS and incubated with secondary antibodies for 1 hour at room temperature. The membranes were then washed with TBS, and antibody binding was detected using the enhanced chemiluminescence system (Piscataway, NJ) and Amersham Hyperfilm MP (Piscataway, NJ). The films were subjected to scanning densitometry to quantitate band intensity by using the NIH Image Software.

3.6. *In vivo* tumor growth assay

Six-week-old female nude mice (NCR/NU) were purchased from Taconic (Cincinnati, OH) and received s.c. injections of KB cells (5×10^6) to the right flank. At 2 weeks, tumors reached 300 mm^3 in volume, and mice were randomized into two experimental groups (n = 10). The treatment group was given 250 mg/kg Coptis chinensis (rhizome). Coptis chinensis was dissolved in water by oral gavage (five times per week) for a period of eight weeks. Mice were weighed, and tumor volume assessed on a weekly basis. Tumor volume was measured by two perpendicular dimensions (long and short) using a caliper and calculated using the formula $(a \times b^2) / 2$, where a is the larger dimension and b is the smaller dimension of the tumor.

3.7. Statistical and bioinformatics analysis

All experiments were performed at least three times. Analysis was done using Minitab statistical software (Minitab, Inc., State College,PA). In order to gain insights into the possible involvement of signaling pathways in Coptis chinensis -induced tumor cells inhibition, bioinformatics pathway analysis was applied to all proteins detected. Pathway analysis was used to find out the significant pathway of the differential genes according to KEGG, Biocarta and Reatome (14,15).The Path-Net was the interaction net of the significant pathways of the expression proteins, and was built according to the interaction among pathways of the KEGG database to find the interaction among the significant pathways directly and systemically. It could summarize the pathway interaction of expression proteins that dealt with Coptis chinensis and found out the reason why a certain pathway was activated (16). Based on lots of interactions of protein-protein and experiment validation, we constructed the interactions repository being a source from KEGG. As distinguished from pathway maps on the KEGG website with respect to interactions of proteins, the repository breakthrough of the protein interactions boundary by pathway class and supplying the integrated protein interactions involved in multiple pathway categories was described. Then, dynamic gene coexpression networks were built according to the

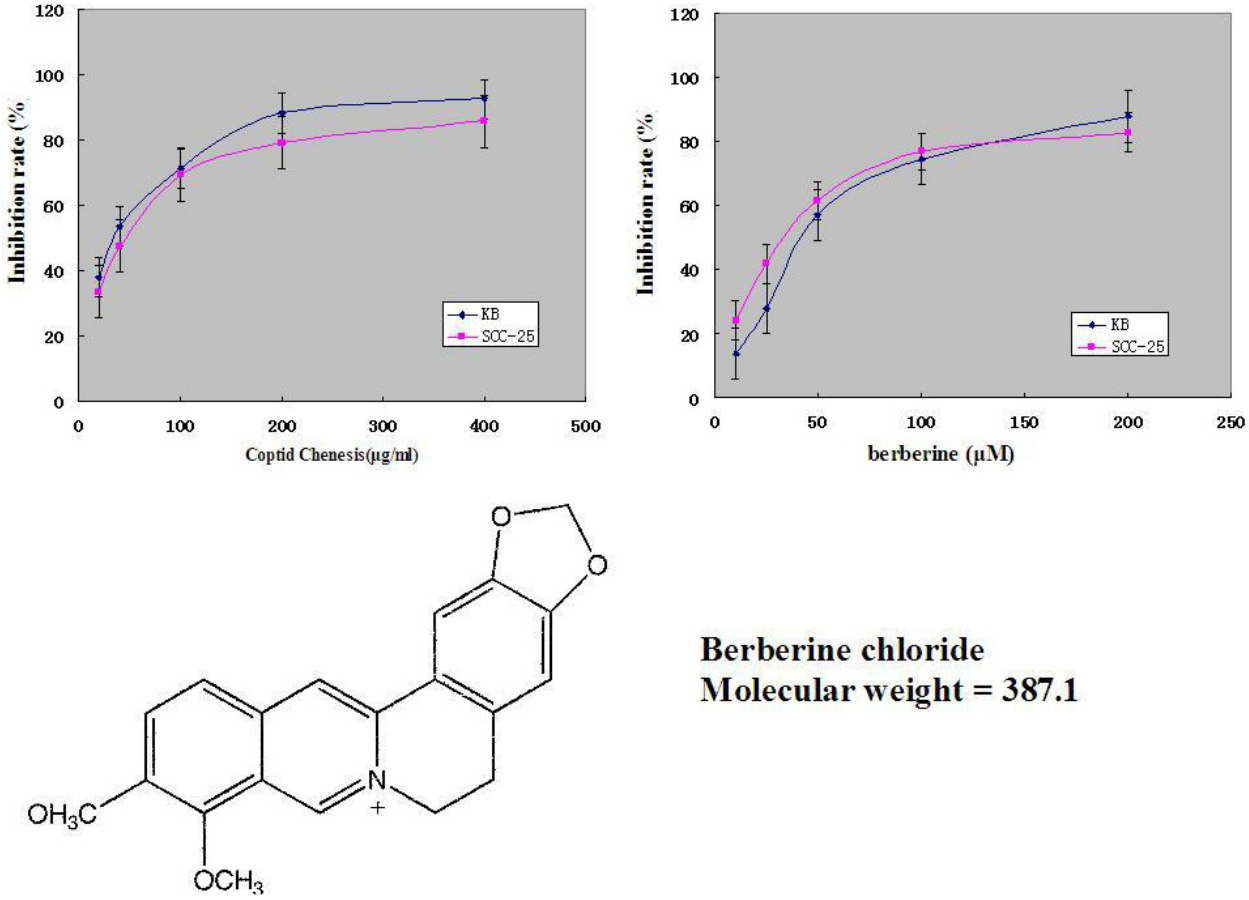

Figure 1. Inhibition of KB and Scc-25 cells growth by Coptis chinensis (A) and Berberine (B). A□B, Cells were seeded onto 96-well plate at 5×10^3 cells/well and were treated at different concentrations. Growth inhibition rate was determined by MTT assay after 48h treatment. A dose-dependent growth inhibition of KB and SCC-25 cells were observed after treatment with Coptis chinensis at concentrations ranging from 20 to 400μg/ml (A) and berberine at concentrations ranging from 10 to 200μM (B). Results are mean values of independent experiments performed in triplicate and with three trials. C, Chemical structure and molecular weight of berberine chloride.

normalized signal intensity of specific expression proteins, in which the centrality of the network was represented by the highest degree in the network.

RESULTS

4.1. MTT assay

To study the effects of Coptis chinensis and berberine on the growth of squamous carcinoma cells, Coptis chinensis and berberine were added at several concentrations to proliferating KB and Scc-25 cells as indicated. The inhibition rate was determined as a percentage of viable treated cells compared with viable control cells. Coptis chinensis and Berberine displayed a dose-dependent growth inhibition in squamous carcinoma cells (Figure 1). After a 48 h treatment with berberine, KB cell viability was reduced to 87.8 % (200 μM), 74.4 % (100μM), 57.2 % (50 μM), 28 % (25 μM), and 13.7 % (10 μM), Scc-25 cell viability was reduced to 82.8 % (200 μM), 76.9 % (100μM), 61.6 % (50 μM), 42 % (25 μM), and 24.3 % (10 μM) separately. All experiments were performed at least three times.

4.2. *In vivo* tumor growth assay

To confirm the anticancer activity of Coptis chinensis, an *in vivo* experiment was carried out. Nude mice were inoculated s.c. with KB cells and were treated with Coptis chinensis by oral gavage at a dose of 250 mg/kg daily. KB cells were used because they grew well in nude mice, whereas Scc-25 grew poorly.

Our results showed that administration of Coptis chinensis significantly reduced the tumor growth in the treated mice as compared with the untreated mice (Figure 2). Average tumor volume at 4 weeks was 1622.8 mm^3 in the treated mice and 5259.3 mm^3 in the control mice. A tumor from one of the treated mice was nonpalpable after 8 weeks of treatment, indicating a complete remission of tumor after the administration of Coptis chinensis.

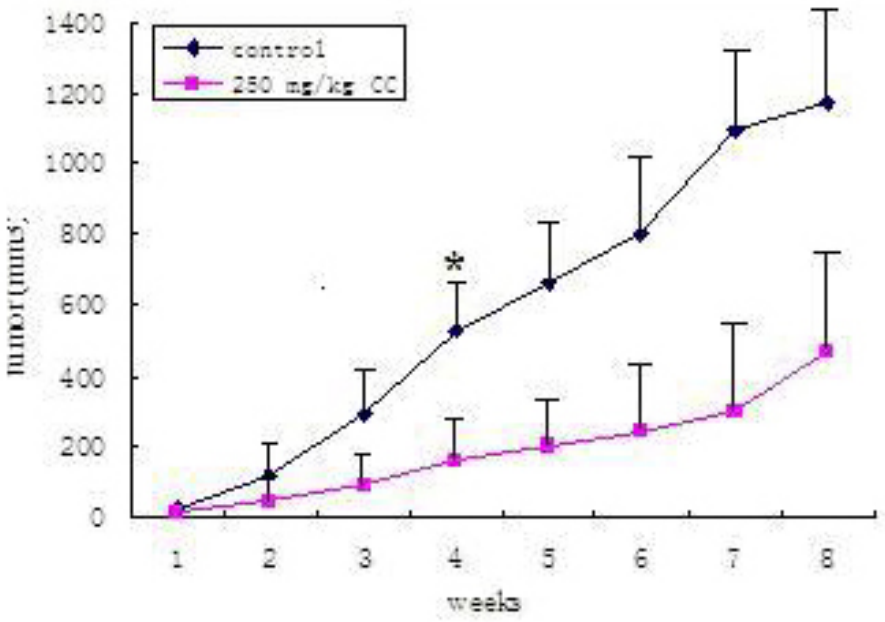

Figure 2. Time-course of tumor growth of mice after treating with Coptis chinensis. Mice were divided into control (n = 10) and Coptis chinensis treatment groups (n = 10). Mice in Coptis chinensis treatment group were treated intragastrically with 250 mg/kg Coptis chinensis once a day. The tumor volume was measured every week throughout the experiment. * $p < 0.01$ (treated vs. control at 4 weeks)

At a dose of 250 mg/kg of Coptis chinensis, no evidence of drug-related toxicity was observed in treated mice by comparing their complete blood count, liver chemistry, or kidney function with those of controls. Therefore, the herb was well tolerated by the animals.

4.3. Pathway Array

4.3.1. Comparison proteins fold-change by Pathway Array

The Pathway Array analysis (Figure 3), using a set of 122 protein and phospho-specific antibodies, revealed that 88 of them were expressed in KB cells, 85 of them were expressed in Scc-25 cells and 35 of them were not expressed in both KB and Scc-25 cells. Those proteins are an active participant in following pathways.

After treatment by Coptis chinensis and berberine, 29 of them changed more than 1.5-fold at the dose of 100μg/ml Coptis chinensis and 100 μM berberine (Table 1). Furthermore, four of them showed a dose dependent decrease (p-ERK, Cdk6, Cdk4, p-RB) and four of them showed dose-dependent increase (p-PKCα, cyclin B1, cyclin E, Osteopontin) in both KB and SCC-25 cells after treating with Coptis chenesis and berberine. These data suggested that Coptis chinensis and berberine have a broad effect on the cell signaling pathways, including cell cycle regulation, DNA synthesis and repair, differentiation, angiogenesis, apoptosis, cell adhesion, cytoskeleton, MAPK signaling, and the phosphatidylinositol 3-kinase signaling pathway. In addition, 21 proteins or phosphorylations (E-cadherin, HIF-2α, Notch 4, p-Akt, Akt, p-PTEN, p-Stat3, cyclin D1, Hsp90, p-CREB, p27, BRCA1, PCNA, c-kit, Raf-1, ERK1/2, p-p38,Cox2, p53, p-PKC α/βII, Vimentin) showed a different change between KB and Scc-25 cells after treatment.

4.3.2. Conventional Western blot analysis

A subset of 6 proteins was selected from Table 1 for validation using conventional Western blotting (one antibody per blot) under conditions that were optimal for each antibody. This method confirmed the Pathway Array results. They included cyclinE, Osteopontin, p-ERK, Cdk6, Cdk4, cyclinB1 (Results not shown).

4.4. Pathway-Analysis

We further performed computational analysis of pathway analysis to find out the significant pathway of the differential genes according to the internet database, such as KEGG (Kyoto Encyclopedia of Genes and Genomes, http://www.genome.jp/kegg/pathway.html), Biocarta (http://www.biocarta.com/genes/index.asp), and Reactome (http://www.reactome.org) (Table 2, Figure 4).

Briefly, Fisher's exact test and χ^2 test were used to classify the pathways or categories associated with the proteins. We computed p values for the Pathways of all expressed proteins, and the false discovery rate (FDR) was calculated to correct the p values. Enrichment provides a measure of the significance of the function: as the enrichment increases, the corresponding function is more specific, which helps us to find those pathways with more concrete function description in the experiment. Within the significant category, the enrichment Re was given by: Re =

Table 1. Differential proteins and their regulation pathway.

Protein	Function	KB		Scc-25	
		CC	Ber	CC	Ber
Cell cycle regulation					
cyclinB1 cyclinD1 cyclinE Cdk6	a subunit for the Cdk1 protein kinase	3.5	2.8	1.6	2.0
Cdk4 P27	regulate the cyclin-dependent kinases Cdk4/6	2.2	3.2	NC	NC
	associate with and activate Cdk 2	1.6	1.8	2.0	2.6
	cyclin-dependent kinase 6	-2.6	-2.2	-1.5	-2.6
	cyclin-dependent kinase 4	-1.8	-1.6	-4.3	-16.7
	a member of cyclin-dependent kinase inhibitors	-2.1	-3.8	NC	NC
Cell adhesion					
E-cadherin Osteopontin	tissue structure and morphogenesis	4.5	2.7	NC	NC
	extracellular matrix adhesion phosphoglycoprotein	1.9	3.1	2.5	3.0
Apoptosis and autophagy					
p53	tumor suppressor genes	NC	NC	-2.6	-3.1
p-Stat3 BRCA 1	membrane receptor signaling	-2.7	-5.9	NC	NC
	cancer susceptibility gene	-5.7	-14.3	NC	NC
MAPK signaling					
Raf-1 p-ERK ERK1/2 p-p38	cytoplasmic protein with serine/threonine activity	-3.4	-16.7	NC	NC
	big mitogen -activated protein kinase 1	-8.0	-3.0	-2.6	-12.1
	dual- specificity protein kinases in MAPK cascade	-1.7	-2.0	NC	NC
	p38 MAP kinase	1.7	3.7	-12.5	-3.0
PI3K/Akt signaling					
P-Akt	the serine /threonine kinase Akt family	-3.3	-4.0	11.8	2.2
Akt	a kinase of PI3K pathway	NC	NC	-2.0	-4.0
p -PTEN	a major negative regulator of the PI3K/Akt	-2.6	-2.0	NC	NC
DNA synthesis and DNA repair					
PCNA	the proliferating cell nuclear antigen	NC	NC	-1.5	-2.6
p-CREB	transcription factor	-1.4	\-2.2	NC	NC
p-RB	retinoblastoma tumor suppressor gene	-1.4	-4.8	-14.3	-3.8
Cytoskeletal signaling					
Vimentin	cytoskeletal intermediate filaments	NC	NC	-5.9	-4.3
p -PKCα	cell growth, differentiation	2.1	2.2	1.6	1.8
p -PKCα/βII	cell growth, differentiation	2.5	1.6	NC	NC
Other cell signaling					
Cox2	prostaglandin synthases	-3.3	-10	NC	NC
Hsp90	heat shock proteins	NC	NC	2.1	12.2
HIF-2α	hypoxia-inducible factors	NC	NC	7.6	28.4
c-kit	proto-oncogene	-2.4	-53.7	NC	NC
Notch4	transmembrane receptors	3.0	2.5	NC	NC

Note: This table presents the summary of results obtained for proteins showing mostly >1.5-fold change (increase or decrease) in KB and Scc-25 cells after treating with Coptis Chinensis (100μg/ml) and berberine (100μM) for 48 hrs. + increased, - decreased, NC - no change.

$(n_f / n) / (N_f / N)$: where n_f is the number of differential proteins within the particular category, n is the total number of proteins within the same category, N_f is the number of differential proteins in the entire array, and N is the total number of proteins in the patharray analysis.

4.4.1. Path-net

The Path-Net was the interaction net of the significant pathways of the expression proteins, and was built according to the interaction among pathways to find the interaction among the significant pathways directly and systemically. It could summarize the pathway interaction of expression proteins that dealt with Coptis chinensis and found out the reason why a certain pathway was activated.

The analysis showed that a wide variety of cellular processes, including MAPK signaling pathway, apoptosis, P53 signaling pathway, cell cycle, adherens junction and cytokine-cytokine receptor interaction, were affected by Coptis chinensis and berberine, further supporting our Pathway Array findings (Figure 5). Based on these analyses, we were able to predict the network of protein-protein interaction that is affected by Coptis chinensis treatment.

4.4.2. Signal expression pathway analysis

Based on lots of interactions of protein-protein, which were validated by experiment, we constructed the interactions repository being a source from KEGG. As distinguished from pathway maps on the KEGG website with respect to interactions of proteins, the repository breakthrough of the protein interactions boundary by pathway class and the supplying of the integrated protein interactions involved in multiply pathway categories was obtained. We can search downstream or upstream proteins or DNA of special protein with the database. If some proteins were defined to be top upstream proteins, the downstream proteins could be defined by iterative search in the repository. We can utilize the iterative search to find the global pathway from proteins located cytoplasm or cytomembrane to transcription factors. Based on the NCBI Chem database, the exact membrane target protein in which berberine combined can be identified. Then, we can derive the interaction among nodes in the pathway network through an iterative search of the KEGG database which is a breakthrough in the limitation of a single pathway. In accordance with the signal pathway map, a sequential three-part protein kinase cascade is initiated through the binding of berberine and a membrane target protein. Upon

Table 2. Difference gene significant pathways

Pathname	*p* value	FDR	enrichment
Pathways in cancer	3.33E-52	8.176E-52	59.3041
Prostate cancer	1.002E-32	1.23E-32	116.76597
Cell cycle	3.387E-28	2.772E-28	83.176513
Glioma	6.219E-26	3.817E-26	124.35077
Melanoma	2.435E-25	1.085E-25	113.84225
Pancreatic cancer	3.019E-25	1.235E-25	112.26111
Chronic myeloid leukemia	5.643E-25	1.97E-25	107.77067
Non-small cell lung cancer	8.107E-25	2.488E-25	138.98995
Small cell lung cancer	4.503E-24	1.228E-24	93.986047
Endometrial cancer	1.052E-22	2.584E-23	133.23297
Focal adhesion	3.245E-22	7.242E-23	45.730127
Acute myeloid leukemia	7.061E-22	1.365E-22	115.46857
MAPK signaling pathway	7.74E-22	1.462E-22	36.21708
Neurotrophin signaling pathway	1.457E-21	2.409E-22	63.644094
Bladder cancer	1.512E-21	2.475E-22	151.20884
p53 signaling pathway	4.395E-21	6.745E-22	100.40745
Colorectal cancer	6.203E-18	8.787E-19	75.604422
ErbB signaling pathway	9.314E-18	1.271E-18	72.997373
T cell receptor signaling pathway	1.116E-16	1.442E-17	58.803439
VEGF signaling pathway	2.165E-16	2.658E-17	75.966165
Renal cell carcinoma	9.832E-15	1.15E-15	74.229796
mTOR signaling pathway	7.586E-14	8.141E-15	88.821978
Thyroid cancer	1.04E-13	1.078E-14	139.35862
Gap junction	1.152E-13	1.178E-14	57.099843
GnRH signaling pathway	3.315E-13	3.256E-14	50.942017
Fc epsilon RI signaling pathway	2.535E-12	2.394E-13	58.465099
Epithelial cell signaling in Helicobacter pylori infection	6.124E-11	5.515E-12	59.432353
Chemokine signaling pathway	1.034E-10	9.013E-12	27.062946
Adhesion junction	1.501E-10	1.262E-11	52.485714
Tight junction	1.878E-10	1.537E-11	34.46823
Apoptosis	4.23E-10	3.35E-11	45.408989
Toll-like receptor signaling pathway	1.039E-09	7.97E-11	40.013861
Adipocytokine signaling pathway	3.982E-09	2.957E-10	51.702345
B cell receptor signaling pathway	7.948E-09	5.655E-10	46.187429
Insulin signaling pathway	9.303E-09	6.526E-10	29.285507
Melanogenesis	5.433E-08	3.662E-09	33.631623
Pathogenic Escherichia coli infection - EHEC	7.252E-08	4.812E-09	54.466307
Dorso-ventral axis formation	2.031E-07	1.312E-08	92.374857
Long-term potentiation	3.447E-07	2.17E-08	40.093254
TGF-beta signaling pathway	8.921E-07	5.476E-08	33.180624
Endocytosis	1.857E-06	1.112E-07	18.52437
Amyotrophic lateral sclerosis (ALS)	5.265E-06	3.06E-07	41.988571
Natural killer cell mediated cytotoxicity	8.436E-06	4.772E-07	21.070907
Wnt signaling pathway	1.4E-05	7.566E-07	18.991541
Jak-STAT signaling pathway	1.54E-05	8.228E-07	18.623963
Long-term depression	1.553E-05	8.291E-07	32.074603
Regulation of actin cytoskeleton	7.598E-05	3.908E-06	13.364418
Leukocyte transendothelial migration	0.0001128	5.673E-06	19.406483
Type II diabetes mellitus	0.0001528	7.509E-06	36.851672
Axon guidance	0.0001543	7.578E-06	17.902104
Mismatch repair	0.0014616	6.765E-05	50.203727
Vascular smooth muscle contraction	0.0021387	9.613E-05	15.061118
Cytokine-cytokine receptor interaction	0.0022949	0.0001025	8.78088
Base excision repair	0.0033915	0.0001447	32.99102
Ubiquitin mediated proteolysis	0.003534	0.0001499	12.642544
DNA replication	0.0035869	0.0001518	32.074603
Prion diseases	0.0035869	0.0001518	32.074603
Nucleotide excision repair	0.0053382	0.0002216	26.242857
Basal cell carcinoma	0.0082775	0.0003332	20.994286

Note: The threshold of significance was defined by *p* value and false discovery rate (FDR) ($p < 0.01$ FDR < 0.01). The enrichment Re was also calculated. All of these proteins show increased enrichment, *p* values, and FDRs.

combination, MAPK1 phosphorylates and activates the transcription factor, including MYC, ETS1, FOS and JUN. Signals are delivered to the nucleus and regulate protein expression through its effects on mRNA. Finally, berberine could impact more than 34 proteins' expression in our experimental data (Figure 6).

4.4.3. Dynamic gene co-expression network

In biology processes, a macromolecular network can be constructed by the experience results such as Y-2H, coimmunoprecipitation (17), or the algorithmic prediction based on the gene function correlation and expression profiles (18). Because of the flexibility of the network model based on the algorithmic prediction from a high throughput test, we can look at snapshots of protein-protein

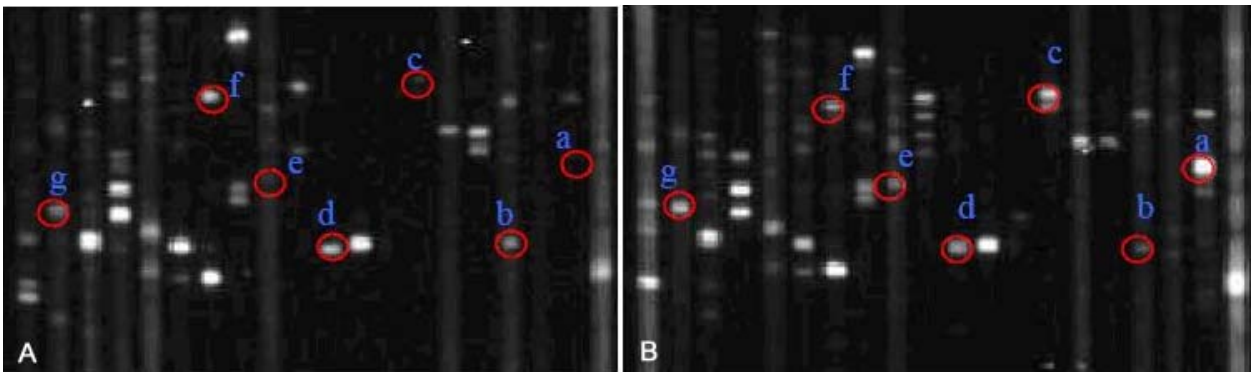

Figure 3. Chemiluminescence images of Pathway Array analysis. This template screens 38 of the 122 different antibody specificities, showing proteins expressed in KB (A) and Scc-25 (B) cells.p53; b) ETS1; c) beta-catenin; d) cdc2 p34; e) Cdc25C; f) cPKCα; g) Cdk6.

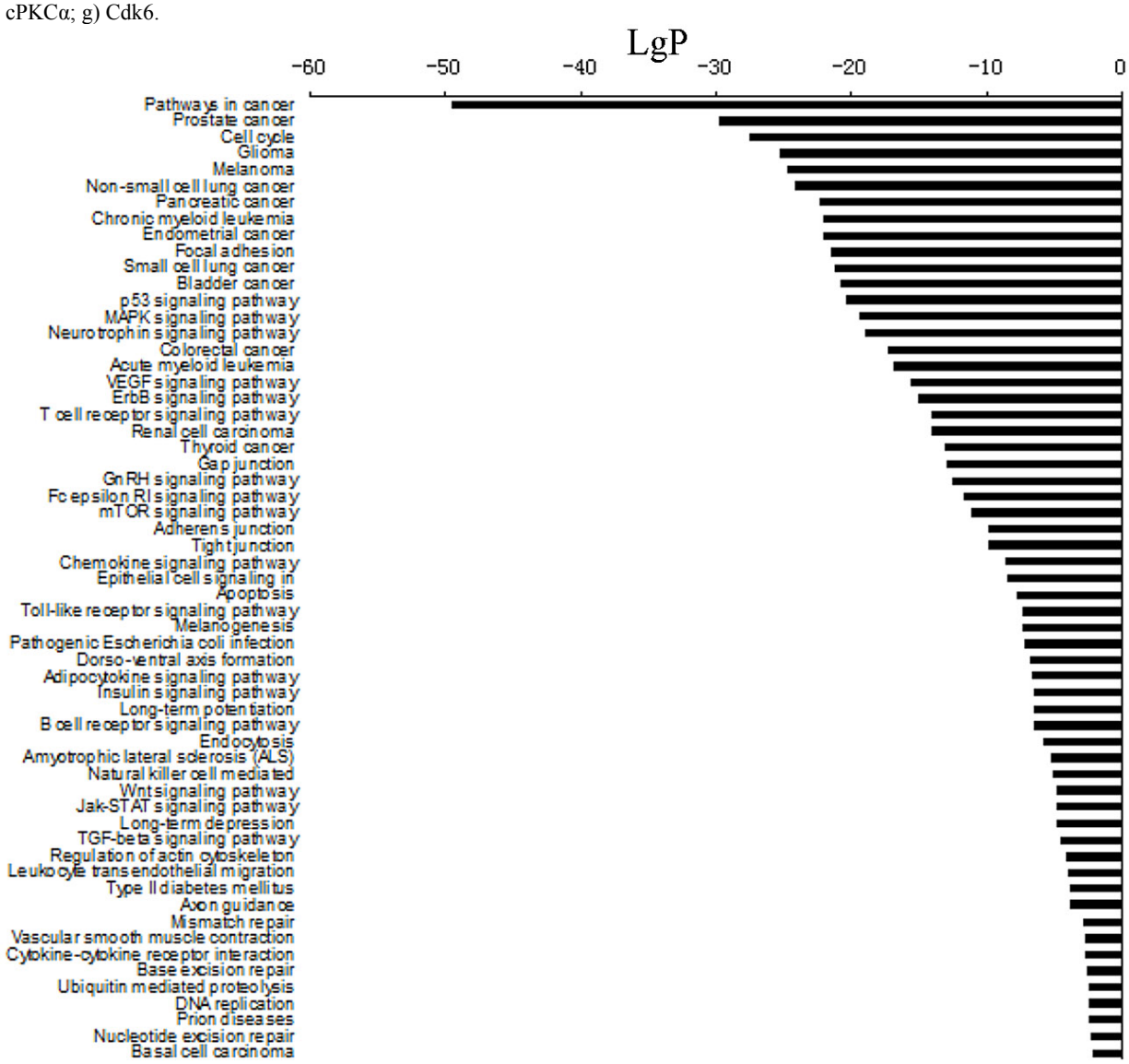

Figure 4. Difference gene significant pathways.

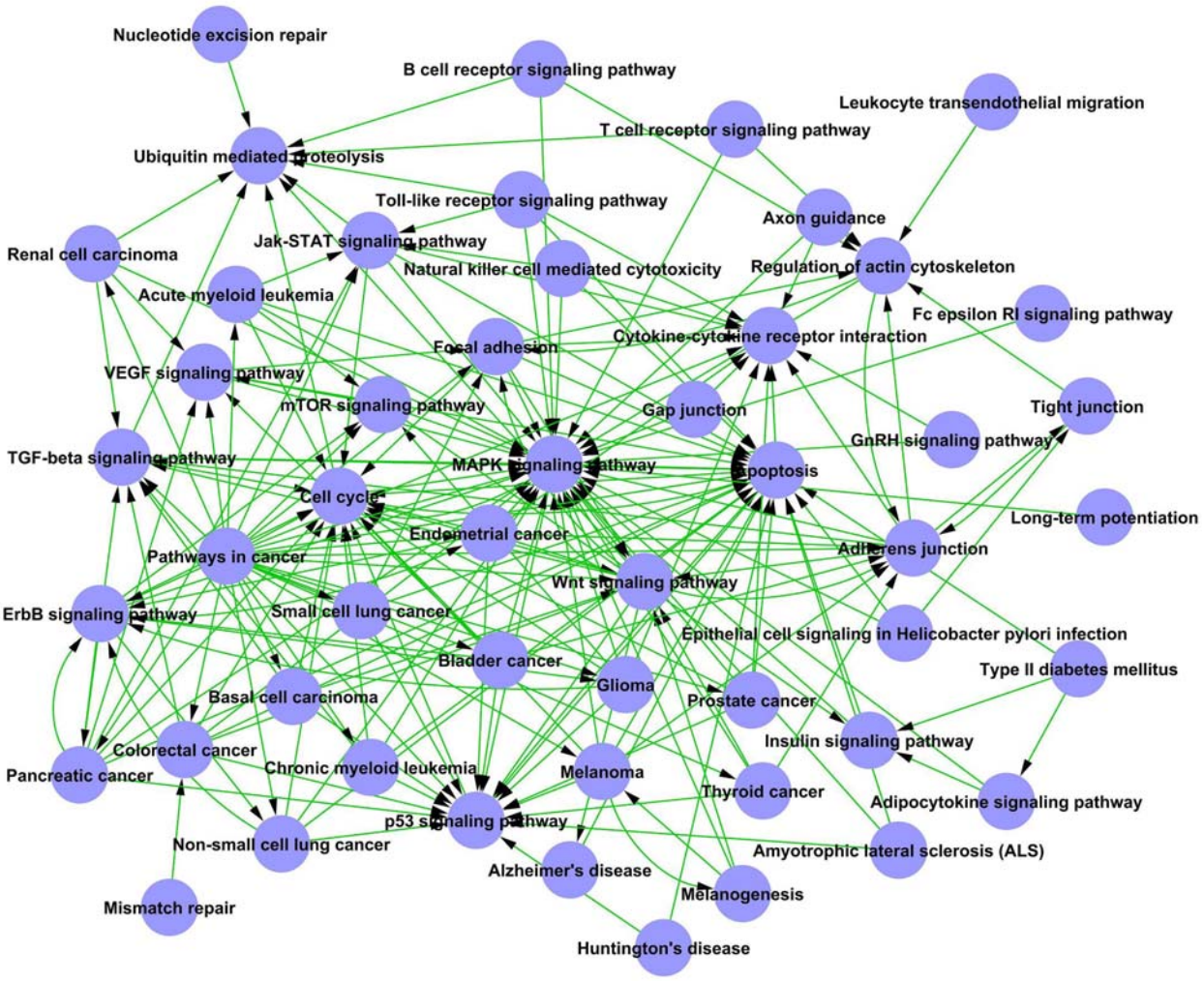

Figure 5. Path-net analysis. Many of these signaling pathways, such as MAPK signaling pathway, apoptosis, P53 signaling pathway, cell cycle, adherens junction and cytokine-cytokine receptor interaction, have been shown to participate in the functionality of Coptis chinensis.

interaction, gene expression regulatory network and metabolism networks among different groups (19).

Within the network analysis, degree centrality is the most simplest and important measures of the centrality of a gene within a network that determine the relative importance. Degree centrality is defined as the link numbers one node has to the other (20). The purpose of network structure analysis is to locate core regulatory factors (genes). In one network, core regulatory factors connect most adjacent genes and have the biggest degrees. As network elements represent a variety of abilities of genes regulating other genes, a large scale gene network can be divided into some subgraph (named i-core network), which all genes are connected to at least k other genes in the subgraph. As a result, the rank of i-core value describes the complexity of the gene association relationship. In the light of the definition of the i-core network, core status within a large scale gene network consists of a higher i-core value subgraph. An i-core subgraph of a graph can be generated by recursively deleting the vertices from the graph whose degree is less than k. The complexity of gene relationship increased with i-core value rank. Larger values of coreness clearly correspond to vertices with larger degree and more central position in the networks structure. For each pair of genes, we calculate the Pearson correlation and choose the significant correlation pairs to construct the network (26).

In this work, we apply the notion of the i-core subgraph to predict gene function similarity (21). To construct two sorts of networks, referred to Coptis chinensis and berberine, we transform the normalized expression value of the Pearson correlation into measures of pair wise connection strengths. Then, we selected genes of the significant differential genes for constructing the co-expression network (Figure 7). The intrinsic gene network of the phenotype can represent the gene function propriety of the sample. Network structure embodying phenotype should collapse without the highest degree gene so that the

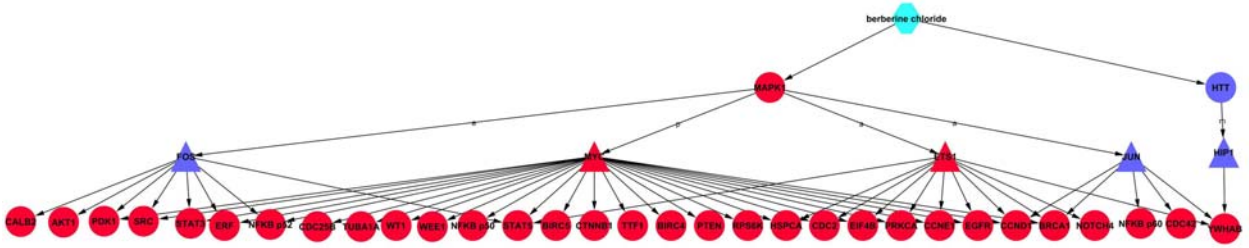

Figure 6. Signal-expression pathways. Red cycle nodes represent proteins, triangular nodes represent transcription factors. Straight lines show interaction of proteins, arrowheads show activated effect, panheads show inhibitory effect. A represents activation, P represents phosphorylation.

biological character should be varied. In addition, another scale of genes within the network (clustering coefficient) estimates complexity of interaction among neighbor genes of the core gene except the participation of core gene. While considering different networks, core regulatory factors were determined by the degree differences between two class samples (22). The centrality of the network is represented by the highest degree in the network (24). It is possible to find the characteristic variables of distances among genes. The core of maximum order is referred to as the main core or the highest i-core of the graph (25).

5. DISCUSSION

In the United States, there are 70,000 newly diagnosed patients with head and neck cancer each year (27). Squamous cell carcinoma is the predominant type. Despite improvements in treatment modalities during the past 40 years, the 5-year survival rate has not dramatically changed. Squamous cell carcinoma is a heterogeneous disease with complex molecular abnormalities. The development and search for more effective therapeutic agents in the treatment of the disease has now become an important subject of research.

Natural herbs have been a continuous source of novel compounds for the treatment of numerous diseases, with natural products and their synthetic derivatives comprising over 60% of the approved anticancer drug candidates developed between 1981 and 2002(28). Coptis chinensis has been shown to have non-toxic effects to humans and have a wide range of pharmacological activities, including anti-microbial effects (29), anti-inflammatory activities (30), the ability to lower cholesterol levels, inhibitory effects on the cyclooxygenase-2 (31) and anti-tumor activities .Wang *et al.* (32) reported that a Coptis Chinensis compound can affect the gene expression in the tissue of an implanted tumor. The growth of several different types of cancer is inhibited by Coptis chinensis, such as lung cancer, melanoma, breast cancer, gastric cancer, and colorectal cancer (33-35). However, the effects of Coptis chinensis on the behavior of squamous cell carcinoma have not yet been established, and the mechanism behind its anti-tumor effects is still unclear.

In this study, we examined the direct impact of Coptis chinensis on the growth of the KB and Scc-25 cells. Since berberine is one of the major active components of Coptis chinensis, we used berberine as a comparison to determine whether the purified molecules of Chinese medicines, in addition to the complex itself having the same effect on cell signaling to better understand the complex phytopharmacology of these drugs and avoid contradictory results. Our data showed that Coptis chinensis and berberine are able to inhibit the growth of squamous carcinoma cells (Figure 1). In xenografted nude mice, administration of Coptis chinensis significantly reduced the tumor growth in the treated mice as compared with the untreated mice (Figure 2). The compound was well tolerated, no evidence of drug-related toxicity was observed by comparing complete blood count, liver chemistry, or kidney function (Figure 3).

In order to understand the global effect of Coptis chinensis on cell signaling, we applied a Pathway Array technology which is an innovative proteomic assay that allows global screening of changes in protein expression and phosphorylation. We compared the levels of proteins in squamous carcinoma cells by high-throughput immunoblotting (Pathway Array) using 122 antibodies, focusing on the proteins and phosphorylation sites altered in cancer cells and functionally linked to proliferation, apoptosis, cell cycle regulation, DNA repair, signaling, and transcription activity. Our results revealed a total of 29 proteins or phosphorylations changing more than 1.5-fold at the dose of 100 μM berberine and 100μg/ml Coptis Chenesis (Table 1). Of these, 4 showed a dose dependent decrease (p-ERK, Cdk6, Cdk4, p-RB) and 4 showed dose-dependent increase (p-PKCα, cyclin B1, cyclin E, Osteopontin) in both KB and SCC-25 cells. In addition, 21 proteins or phosphorylations (p-PKC α/βII, p-p38, E-cadherin, HIF-2α, Notch 4, p-AKT, p-Stat3, cyclin D1, Hsp90, p-PTEN, ERK1/2, p-CREB, p27, BRCA1, PCNA, Akt, c-kit, Raf-1, Cox2, p53, Vimentin) showed a different change between KB and Scc-25 cells after treatment. These results reflected that squamous carcinoma is a heterogeneous cancer and their response to drugs is different. However, the majority of proteins or phospho-proteins that were affected by berberine and Coptis chinensis were cell cycle regulatory factors, nuclear proteins, MAPK signaling and PI3K signaling, etc. These data suggested that Coptis chinensis and berberine have a broad effect on the cell signaling pathways. The effect on these factors may be direct or indirect. Conventional Western blotting confirmed some of these changes.

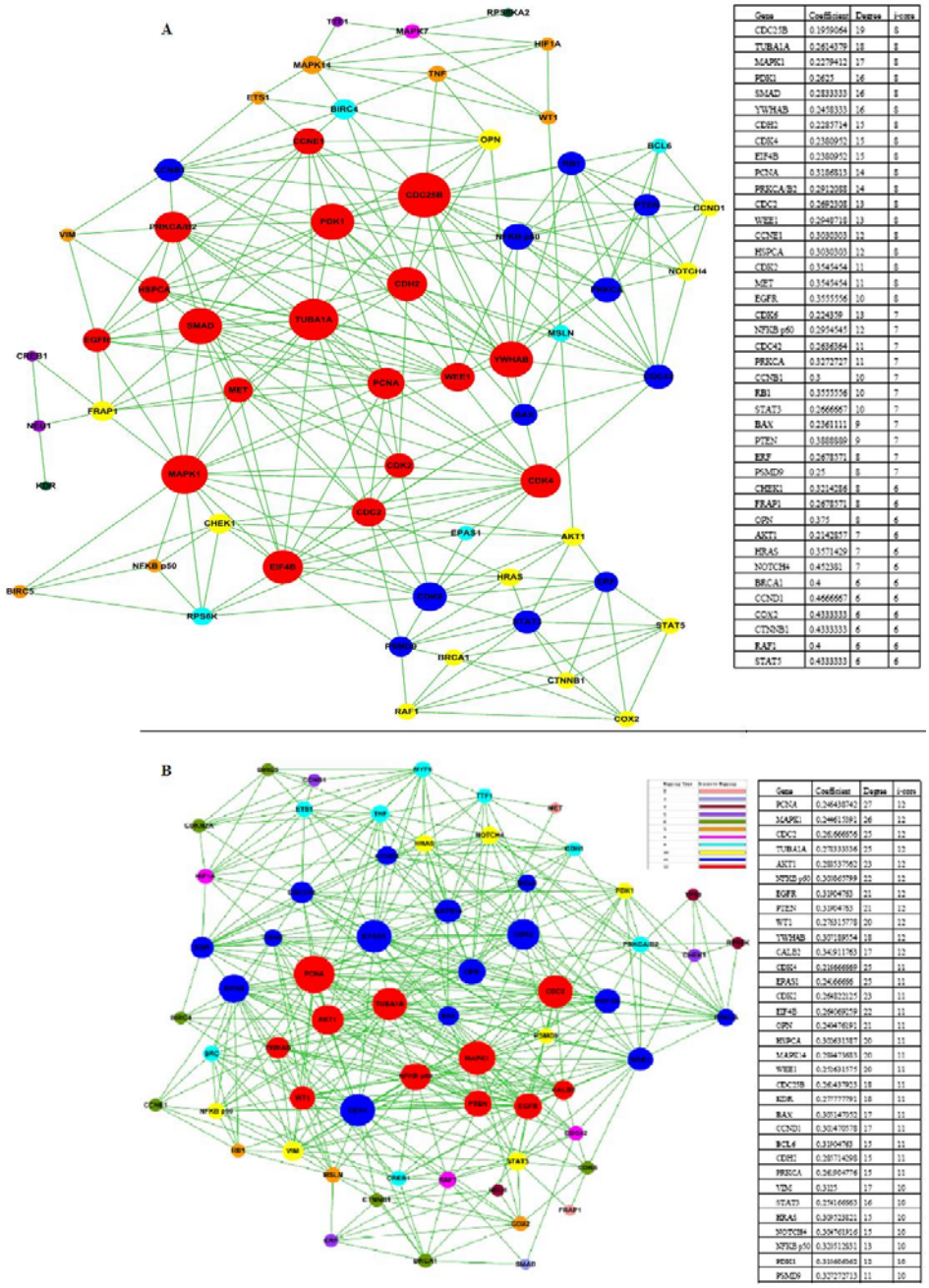

Figure 7. Gene association network. Nodes denote genes, and undirected links denote gene-gene interrelation. The size of nodes represents the power of the interrelation among the nodes. The power is quantized with the degree which is the number of relationship of one gene with others. Genes with larger degree get more relations with others. Different colors of nodes represent distinct i-core gene class. Gene coexpression networks were built according to the normalized signal intensity of specific expression genes. Cycles with identical color lie on the same subgraph. According to the degree distribution of genes in the normal sample network, we identified the core regulatory genes. A, Dynamic Gene Networks in KB cells after berberine treatment for 48h with highest i-coreness value and degree including: CDC25B, TUBA1A,MAPK1,PDK1,SMAD,YWHAB; B, Dynamic Gene Networks in KB cells after Coptis chinensis treatment for 48h with highest i-coreness value and degree including: PCNA,MAPK1,CDC2, TUBA1A. Clustering coefficient and degree describe the network propriety of genes. I-core represents the subnetwork of which genes locate. As shown in the table, the less clustering coefficient that exists, the more independence of core gene interaction among neighbor genes of core gene. Degree within the network describes the number of one gene regulating other ones, which represents the size of the cycle node. The higher degree, the nearer the gene is located within the network.

Table 3. Comparison of networks structure between KB coptis48h and KB coptis48h

Sample	Weighted Clustering Coefficient	Density
KB coptis48h	0.283	0.112
KB ber48h	0.281	0.075

Table 4. Variance Analysis of co-expression network between Coptis chinensis and berberine

protein	CC Clustering Coefficient	CC Degree	CC kcore	Ber Clustering Coefficient	Ber Degree	ber kcore	dif-Clustering Coefficient	dif-Degree	dif-kcore
EPAS1	0.242	25	11	0.350	5	5	-0.108	20	6
KDR	0.278	18	11		1	1	0.278	17	10
AKT1	0.289	23	12	0.214	7	6	0.074	16	6
WT1	0.276	20	12	0.250	5	4	0.026	15	8
MAPK14	0.289	20	11	0.190	7	4	0.099	13	7
MYF6	0.301	13	9	0.000	0	0	0.301	13	9
OPN	0.240	21	11	0.375	8	6	-0.135	13	5
PCNA	0.246	27	12	0.319	14	8	-0.072	13	4
VIM	0.313	17	10	0.333	4	4	-0.021	13	6
CCNE1	0.433	6	6	0.303	12	8	0.130	-6	-2
CDK6	0.310	7	6	0.224	13	7	0.085	-6	-1
FRAP1	0.500	2	2	0.268	8	6	0.232	-6	-4
STAT5	0.000	0	0	0.433	6	6	-0.433	-6	-6
MET	0.500	2	2	0.355	11	8	0.145	-9	-6
SMAD	0.333	3	3	0.283	16	8	0.050	-13	-5

There are several reports in agreement with our results. Li *et al.* (33) reported that Huanglian represents a class of agents that can inhibit tumor cell growth by directly suppressing the expression of a cyclin subunit that is critical for cell cycle progression. Berberine-induced anti-proliferative effects against prostate carcinoma cells was associated with G1-phase arrest that correlated with inhibition of expression of cyclins D1, D2 and E; cyclin dependent kinases (Cdk) 2, Cdk4 and Cdk6; and increased expression of Cdk inhibitory proteins $p21^{Cip1}$ and $p27^{Kip1}$ (36). Luo *et al.* (37) reported berberine inhibits cyclin D1 expression via suppressed binding of AP-1 transcription factors to CCND1 AP-1 motif, which is probably one of the important mechanisms behind the anti-tumor effects of berberine as a regulator of cyclin D1. Lin *et al.* (38) found that berberine induces G2/M-phase arrest through signaling of wee1, 14-3-3sigma, Cdc25c, CDK1, and cyclin B1 in leukemia cells. Together with these reports, our results suggest that the effects of berberine treatment in squamous carcinoma cells rely upon the induction of the cell cycle arrest and apoptosis. Hsu *et al.* reported (39) that berberine may play an apoptotic cascade in SW620 cells by activation of the JNK/p38 pathway and induction of ROS production, providing a new mechanism for berberine-induced cell death in human colon cancer cells. Jantova *et al.* (40) found that berberine induced G(0)/G(1) cell cycle arrest and apoptosis in L1210 cells. Mantena *et al.* (12) reported that berberine induced G1 arrest through the Cdki-Cdk-cyclin cascade, and induced apoptosis through the disruption of mitochondrial membrane potential and the cleavage of caspase-3 and PARP in human epidermoid carcinoma A431 cells.

In today's post-genomic era, the sequencing projects and the development of High Throughput (HTP) technologies such as microarray and proteomics provide great opportunities to uncover and explore the complexity of biological problems using systems biology. Analysis of High Throughput (HTP) Data, such as microarray and proteomics data, has provided a powerful methodology to study patterns of gene regulation on a genome scale. A major unresolved problem in the post-genomic era is to assemble the large amounts of data generated into a meaningful biological context. A variety of software tools are available to extract and analyze HTP data that primarily focus on microarray data. Many software tools capable of analyzing HTP data within the context of biological pathways have been developed (41,42).

It is important to note that the proteins identified in this study do not act independently to inhibit cell proliferation but rather as part of a complex signaling network. To better understand the protein-protein interaction network in squamous carcinoma cells as well as the effect of Coptis chinensis on this network, Pathway analysis was used to find out the significant pathway of the differential genes. The Path-Net was the interaction net of the significant pathways of the differential expression proteins, and was built according to the interaction among pathways of the KEGG database to find the interaction among the significant pathways directly and systemically. It could summarize the pathway interaction of differential expression genes under actions of Coptis chinensis and berberine, which described the reason why a certain pathway was activated.

To evaluate difference of protein-protein interaction between Coptis chinensis and berberine treatment with insight on whole interaction networks, we compared two arguments of network structure including density and cluster coefficient between Fig 7A and Fig 7B. The network of Fig 7B possessed much more interactions than Fig 7A, according to comparison of density. However, proteins in two networks had similar capability of interactions independently on center regulatory genes based on comparison of the cluster coefficient (Table 3). We speculate that berberine, the major active component of Coptis chinensis, has the similar therapeutic effectiveness with Coptis chinensis. However, other unknown ingredients of Coptis chinensis could also activate genes in the network

to achieve positive ajuvant effectiveness (Table 4). For example, both EPAS1 and KDR are not the downstream effectors of berberine, but they were activated after treatment by Coptis chinensis and participated in the regulation in this network. AKT1, one of the immediate effectors of berberine, exhibited more powerful co-expression capability after treatment by Coptis chinenesis in comparison with berberine, which indicate that other unknown ingredients of Coptis chinensis have a synergetic effect with berberine to enhance its effect. This also exists in WT1. However, SMAD, MET gene, while not under the direct effects of berberine genes, showed higher network characteristics (degree is 16, i-core is 8) when the monomer was used with berberine treatment, This shows that berberine can act, indirectly, as the role of activator of these genes and as a direct effect of berberine on gene co-expression, but the other stereotypes Coptis branch to control this kind of expression.

Our experiments yielded two main findings. Firstly, Coptis chinensis significantly inhibits the growth of squamous carcinoma cells, in a dose-dependent fashion. Moreover, Coptis chinensis has a wide effect on cell signaling, these proteins are involved in MAPK signaling pathway, apoptosis, P53 signaling pathway, cell cycle, adherens junction and cytokine-cytokine receptor interaction signaling pathway. In conclusion, we have demonstrated that it is possible that Coptis chinensis may be used as novel natural anticancer drug to effectively fight against squamous carcinoma cells.

6. ACKNOWLEDGEMENTS

This work was supported by: 1. Leading academic discipline project of Shanghai Municipal Education Committee, Project Number: J50208; 2. Shanghai Municipal Natural Science Foundation.

7. REFERENCES

1. Rojsanga, P., Gritsanapan, W., and Suntornsuk, L.. Determination of berberine content in the stem extracts of Coscinium fenestratum by TLC densitometry. *Med Princ Pract*, 15:373–8. (2006)

2. Ivanovska N, and Philipov S. Study on the anti-inflammatory action of Berberis vulgaris root extract, alkaloid fractions and pure alkaloids. *Int J Immunopharmacol*, 18: 553–61. (1996)

3. Hoshi, A., Ikekawa, T., Ikeda, Y., Shirakawa, S., and Iigo, M.. Antitumor activity of berberine derivatives. *Gann*, 67(2): 321-51. (1976)

4. X-N WANG, L-N XU, J-Y PENG, K-X LIU, L-H ZHANG, and Y-K ZHANG. *In vivo* inhibition of S180 tumors by the synergistic effect of the Chinese medicinal herbs Coptis chinensis and Evodia rutaecarpa. *Planta Med*, 75(11):1215-20. (2009)

5. Auyeung KK, and Ko JK. Coptis chinensis inhibits hepatocellular carcinoma cell growth through nonsteroidal anti-inflammatory drug-activated gene activation. *Int J Mol Med*, 24(4):571-7. (2009)

6. Iizuka, N., Miyamoto, K., Hazama, S., Yoshino, S., Yoshimura, K., Okita, K., Fukumoto, T., Yamamoto, S., Tangoku, A., and Oka, M., Anticachectic effects of Coptidis rhizoma, an anti-inflammatory herb, on esophageal cancer cells that produce interleukin 6. *Cancer Lett*, 158(1):35-41. (2000)

7. C-Y Ma, S-C Shen, D-W Huang, H-M Chang, and JS-B Wu. Growth inhibition and induction of apoptosis in U937 cells by Coptis chinensis extract. *J Food Sci*, 73(6):H127-33. (2008)

8. H-L Lin, T-Y Liu, C-W Wu and C-W Chi1. Berberine modulates expression of mdr1 gene product and the responses of digestive track cancer cells to Paclitaxel. *Br J Cancer*, 81(3): 416 -22. (1999)

9. Kim JB, Yu JH, Ko E, Lee KW, Song AK, Park SY, Shin I, Han W, and Noh DY. The alkaloid Berberine inhibits the growth of Anoikis-resistant MCF-7 and MDA-MB-231 breast cancer cell lines by inducing cell cycle arrest. *Phytomedicine*, [Epub ahead of print] (2009)

10. Fukuda, K., Hibiya, Y., Mutoh, M., Koshiji, M., Akao, S., and Fujiwara, H. Inhibition by berberine of cyclooxygenase-2 transcriptional activity in human colon cancer cells. *J Ethnopharmacol,* 66 (2): 227-33. (1999)

11. Peng PL, Hsieh YS, Wang CJ, Hsu JL, Chou FP. Inhibitory effect of berberine on the invasion of human lung cancer cells via decreased productions of urokinase plasminogen activator and matrix metalloproteinase-2. *Toxicol Appl Pharmacol*, 214: 8–15. (2006)

12. Sudheer K. Mantena, Som D. Sharma, and Santosh K. Katiyar. Berberine, a natural product, induces G1-phase cell cycle arrest and caspase-3-dependent apoptosis in human prostate carcinoma cells. *Mol Cancer Ther,* 5(2):296–308. (2006)

13. Tseng-Hsi Lin, Hsing-Chun Kuo, Fen-Pi Chou and Fung-Jou Lu. Berberine enhances inhibition of glioma tumor cell migration and invasiveness mediated by arsenic trioxide. *BMC Cancer*, 8:58. (2008)

14. Kanehisa, M., S. Goto, S. Kawashima, Y. Okuno, and M. Hattori. The KEGG resource for deciphering the genome. *Nucleic Acids Res,* 32: D277-80. (2004)

15. Draghici, S., P. Khatri, A.L. Tarca, K. Amin, A. Done, C. Voichita, C. Georgescu, and R. Romero. A systems biology approach for pathway level analysis. *Genome Res,* 17: 1537-45. (2007)

16. Yi, M., Horton J.D., Cohen J.C., Hobbs H.H., and Stephens R.M.. WholePathwayScope: a comprehensive pathway-based analysis tool for high-throughput data. *BMC Bioinformatics,* 7: 30. (2006)

17. Smidtas, S., Yartseva, A., Schachter, V., and Kepes, F.. Model of interactions in biology and application to heterogeneous network in yeast. *C R Biol*, 329(12):945–52. (2006)

18. Nikiforova, V. J., and Willmitzer L.. Network visualization and network analysis. *EXS*, 97:245–75. (2007)

19. Carlson, M. R., Zhang, B., Fang, Z., Mischel, P. S., Horvath, S., and Nelson, S. F.. Gene connectivity, function, and sequence conservation: predictions from modular yeast co-expression networks. *BMC Genomics*, 7:40. (2006)

20. Barabasi, A.L. and Oltvai, Z.N.. Network biology: understanding the cell's functional organization. *Nat Rev Genet,* 5: 101-13. (2004)

21. Altaf-Ul-Amin, M., Shinbo, Y., Mihara, K., Kurokawa, K., and Kanaya, S.. Development and implementation of an algorithm for detection of protein complexes in large interaction networks. *BMC Bioinformatics*, 7:207. (2006)

22. Carlson, M.R., Zhang, B., Fang, Z., Mischel, P.S., Horvath, S., and Nelson, S.F.. Gene connectivity, function, and sequence conservation: predictions from modular yeast co-expression networks. *BMC Genomics,* 7: 40. (2006)

24. Barabasi, A. L. and Oltvai, Z. N.. Network biology: understanding the cell's functional organization. *Nat Rev Genet,* 5(2):101–13, (2004)

25. Huber, W., Carey, V. J., Long, L., Falcon, S., and Gentleman, R.. Graphs in molecular biology. *BMC Bioinformatics*, 8 Suppl 6:S8, (2007)

26. Prieto, C., A. Risueno, C. Fontanillo, and J. De las Rivas. Human gene coexpression landscape: confident network derived from tissue transcriptomic profiles. *PLoS One,* 3: e3911. (2008)

27. American Cancer Society, Cancer facts and figures 1997. Atlanta, GA: American Cancer Society, (2002)

28. Newman, D.J., Cragg, G.M., Snader, K.M.. Natural products as sources of new drugs over the period 1981–2002. *J Nat Prod*, 66:1022–37. (2003)

29. Lee S, Lim HJ, Park HY, Lee KS, Park JH, and Jang Y. Berberine inhibits rat vascular smooth muscle cell proliferation and migration *in vitro* and improves neointima formation after balloon injury *in vivo*. Berberine improves neointima formation in a rat model. *Atherosclerosis*, 186: 29–37. (2006)

30. Kuo CL, Chi CW, and Liu TY. The anti-inflammatory potential of berberine *in vitro* and *in vivo*. *Cancer Lett*, 203:127–37. (2004)

31. Kuo CL,Chi CW, and Liu TY. Modulation of apoptosis by berberine through inhibition of cyclooxygenase-2 and Mcl-1 expression in oral cancer cells. *In vivo*, 19: 247–52. (2005)

32. Wang GP, Tang FQ, Zhou JP. Effect of Coptis Chinensis compound on the gene expression in transplanted tumor tissue in nasopharyngeal carcinoma cell line of CNE1 by cDNA microarray. *Hunan Yi Ke Da Xue Xue Bao*, 28(4):347-52. (2003)

33. Xiao-Kui Li, Monica Motwani, William Tong, William Bornmann, and Gary K. Schwartz. Huanglian, A Chinese Herbal Extract, Inhibits Cell Growth by Suppressing the Expression of Cyclin B1 and Inhibiting CDC2 Kinase Activity in Human Cancer Cells. *Mol Pharmacol*, 58: 1287-93. (2000)

34. Gonc¸alo C. Pereira, Ana F. Branco, Ju´lio A. C. Matos, Sandro L. Pereira, Donna Parke,Edward L. Perkins, Teresa L. Serafim, Vilma A. Sardao, Maria S. Santos,Antonio J. M. Moreno, Jon Holy, and Paulo J. Oliveira. Mitochondrially Targeted Effects of Berberine on K1735-M2 Mouse Melanoma Cells: Comparison with Direct Effects on Isolated Mitochondrial Fractions. *JPET*, 323(2):636–49. (2007)

35. Rojsanga Piyanuch, Mugdha Sukhthankar, Gritsanapan Wandee, and Seung Joon Baek. Berberine, a natural isoquinoline alkaloid, induces NAG-1 and ATF3 expression in human colorectal cancer cells. *Cancer Letters*, 258:230–40. (2007)

36. Sudheer K. Mantena, Som D. Sharma, and Santosh K. Katiyar. Berberine, a natural product, induces G1-phase cell cycle arrest and caspase-3-dependent apoptosis in human prostate carcinoma cells. *Mol Cancer Ther*, 5(2):296–308. (2006)

37. Ye Luo, Yu Hao, Tai-ping Shi, Wei-wei Deng, Na Li. Berberine inhibits cyclin D1 expression via suppressed binding of AP-1 transcription factors to CCND1 AP-1 motif. *Acta Pharmacologica Sinica*, 29 (5): 628-33. (2008)

38. Lin CC, Lin SY, Chung JG, Lin JP, Chen GW, and Kao ST. Down-regulation of cyclin B1 and up-regulation of Wee1 by berberine promotes entry of leukemia cells into the G2/M-phase of the cell cycle. *Anticancer Res*, 26: 1097–104. (2006)

39. Hsu WH, Hsieh YS, Kuo HC, Teng CY, Huang HI, Wang CJ, Yang SF, Liou YS, and Kuo WH. Berberine induces apoptosis in SW620 human colonic carcinoma cells through generation of reactive oxygen species and activation of JNK/p38 MAPK and FasL. *Arch Toxicol*, 81:719–28. (2007)

40. Jantova S, Cipak L, Cernakova M, *et al.* Effect of berberine on proliferation, cell cycle and apoptosis in HeLa and L1210 cells. *J Pharm Pharmacol*, 55: 1143–9. (2003)

41. Karp PD, Krummenacker M, Paley S, and Wagg J. Integrated pathway-genome databases and their role in drug discovery. *Trends Biotechnol*, 17:275–81. (1999)

42. Karp PD, Riley M, Paley SM, and Pellegrini-Toole A. The MetaCyc Database. *Nucleic Acids Res*, 30: 59–61. (2002)

Key Words: Coptis chinensis; Berberine; Signaling network; Chinese medicine

Send correspondence to: David Y Zhang, Mount Sinai School of Medicine,New York University, USA, Tel: 212-518-3814, Fax: 212-427-2082, E-mail: david.zhang@mssm.edu

http://www.bioscience.org/current/volE3.htm